IV International Conference on Computational Methods for Coupled Problems in Science and Engineering
COUPLED PROBLEMS 2011
M. Papadrakakis, E. Oñate and B. Schrefler (Eds)

MULTI-LEVEL AND QUASI-NEWTON ACCELERATION FOR STRONGLY COUPLED PARTITIONED FLUID-STRUCTURE INTERACTION

J.J. KREEFT*, M. WEGHS, A.H. VAN ZUIJLEN AND H. BIJL

*Faculty of Aerospace Engineering, Delft University of Technology
Kluyverweg 1, 2629 HS, Delft, The Netherlands
e-mail: j.j.kreeft@tudelft.nl

Key words: Fluid-structure interaction, reduced order modeling, quasi-Newton coupling, multi-level acceleration, adaptivity.

Abstract. Two reduced order models are presented for the simulation of physically strong coupled fluid-structure interaction problem, based on computationally partitioned flow and structure solvers. The reduced order models used are a class of quasi-Newton coupling methods to obtain a stable solution and to reduce the number of subiterations. The second reduced order model is a multi-level acceleration in with coarse grid computations are performed in order to reduce computational costs. Finally an adaptive multi-level strategy is described, that contains an indicator for when to switch from coarse to fine grid level and vice versa.

1 INTRODUCTION

Fluid-structure interaction (FSI) is the interaction between a moving or deformable structure with a fluid flow. Due to the advances in computer power and numerical algorithms we are able to simulate increasingly complex problems. Despite these advances, issues in efficiency and stability of certain FSI problems remain. This is especially apparent in the simulation of physically strong interaction between the flow and structure, using a computationally partitioned coupling method.

The main advantages of the partitioned approach above the monolithic approach is that it allows reusing of existing flow and structure solvers, that are often already developed separately in the past. The main drawback of the partitioned approach over the monolithic approach is that the interface conditions,

$$\vec{v}_f = \frac{\partial \vec{d}_s}{\partial t}, \quad \sigma_f \cdot \vec{n} = \sigma_s \cdot \vec{n}, \quad \text{on } \Gamma_I, \tag{1}$$

are not satisfied automatically. A mismatch in interface conditions in the partitioned approach will eventually lead to stability problems in case of strong physical interaction.

Subiterations are therefore introduced in order to satisfy conditions (1). Because in the partitioned approach the solvers are considered to be blackboxes, a class of reduced order models will be used, called quasi-Newton subiterations, to stabilize the subiteration routine. Examples of these reduced order models that will be summarized here are, in order of increasing complexity, stability and efficiency: the classical Gauss-Seidel method, Aitken's adaptive underrelaxation method [6] and the least-squares method [2]. Other methods that belong to the class mentioned before, that are not discussed in this work, are Interface-GMRES(R) [1] or Newton-Krylov method [7]. It is shown that these are usually outperformed by the least-squares method [2, 5].

Obtaining stability by means of subiterations comes at the cost of a substantial increase in computation times, which depends heavily on the type of quasi-Newton method chosen. A second reduced order model will be introduced to suppress computational costs, i.e. a multi-level acceleration technique, [10], for reducing the costs of the solvers individually. This is especially of interest for the flow solver, which usually takes up most of the computation time. The multi-level acceleration technique discussed here is a coarse grid prediction method. It relies on a solve at the coarse grid level to predict the state at the fine grid level. Coarse grid levels are sufficient for stability, because it are the lower modes that might cause instabilities, and therefore need to be suppressed by the subiterations, [3]. Several strategies are possible with this multi-level acceleration method. One is to first subiterate on the coarse grid until certain convergence criteria is met, and then subiterate on the fine grid level. Alternatively, we can alternate coarse grid and fine grid level solves using a given pattern, e.g. two coarse grid solves followed by one fine grid solve. Finally we present an adaptive multi-level method, which automatically switches between coarse and fine grid level, based on a multi-level ratio criteria. It will be shown that this method significantly reduces the number of fine grid solves, at the cost of a small increase in total number of subiterations.

2 QUASI-NEWTON METHODS

In case of a Dirichlet-Neumann decomposition of the FSI problem, the stress distribution $\mathbf{p}$ on the fluid-structure interface is passed from the flow solver $\mathcal{F}$ to the structure solver $\mathcal{S}$ and the displacement of the interface $\mathbf{d}$ is transferred the other way around.
We consider the flow and structure solver as two black boxes that must be coupled in some way. The flow solver gets as an input the structural displacement and has as an output the fluid stresses acting on the interface. For the structure solver we get vice versa. In equations this becomes

$$\mathbf{d} = \mathcal{S}(\mathbf{p}), \tag{2}$$

$$\mathbf{p} = \mathcal{F}(\mathbf{d}). \tag{3}$$

2.1 Quasi-Newton formulation

In many applications the interaction between fluid and structure is weak, e.g. in aeroelastic problems. These problems can be solved with so-called loosely coupled methods, [4, 8, 11]. Loosely coupled methods consist of a single solve per time-step. These algorithms do not enforce equilibrium on the fluid-structure interface and are therefore often unstable in cases with strong interaction (where density and stiffeness ratios are of the same order). The errors made can diverge for more strong interactions. One way to stabilize the coupling of the partitioned system is to make use of subiterations.

In case we solve (2) and (3) sequentially, it can be writen in a fixed-point formulation,

$$\mathbf{p} = \mathcal{F} \circ \mathcal{S}(\mathbf{p}), \tag{4}$$

so what goes in must come out in order to have equilibrium at the interface. Alternatively this can be written as a residual problem,

$$\mathcal{R}(\mathbf{p}) \equiv \mathcal{F} \circ \mathcal{S}(\mathbf{p}) - \mathbf{p} = 0, \tag{5}$$

where $\mathcal{R}$ is the residual operator of the coupled problem. A popular method to solve a nonlinear system, $\mathcal{R}(\mathbf{p}) = 0$, in dynamical problems is to use Newton's method, so solve the system (with $\mathbf{r}^k = \mathcal{R}(\mathbf{p}^k)$):

$$\left.\frac{\mathrm{d}\mathcal{R}}{\mathrm{d}\mathbf{p}}\right|_{\mathbf{p}^k} \Delta\mathbf{p}^k = -\mathbf{r}^k, \tag{6a}$$

$$\mathbf{p}^{k+1} = \mathbf{p}^k + \Delta\mathbf{p}^k. \tag{6b}$$

However, when using blackbox solvers the exact Jacobian of $\mathcal{R}$ is in general unknown as the derivatives of $\mathcal{F}$ and $\mathcal{S}$ w.r.t. $\mathbf{d}$ and $\mathbf{p}$ are often unavailable, especially the cross derivatives $\partial\mathcal{F}/\partial\mathbf{d}$ and $\partial\mathcal{S}/\partial\mathbf{p}$. The Jacobian must be approximated instead.

First note however that instead of solving (6), using an approximate Jacobian, it is also possible, and much cheaper, to use the following explicit expression,

$$\mathbf{p}^{k+1} = \mathbf{p}^k + \overline{\left(\left.\frac{\mathrm{d}\mathcal{R}}{\mathrm{d}\mathbf{p}}\right|_{\mathbf{p}^k}\right)^{-1}}(-\mathbf{r}^k), \tag{7}$$

where we need an approximation for the inverse of the Jacobian instead. Equation (7) is much cheaper than (6), because (6) requires to solve a dense linear system, where as (7) only uses a matrix vector product. The residual in (7) is calculated as

$$\mathbf{r}^k = \mathcal{R}(\mathbf{p}^k) = \mathcal{F} \circ \mathcal{S}(\mathbf{p}^k) - \mathbf{p}^k = \tilde{\mathbf{p}}^{k+1} - \mathbf{p}^k, \tag{8}$$

with convergence criteria $||\mathbf{r}^k||_2 \leq \epsilon$. This equation shows that $\tilde{\mathbf{p}}^{k+1} = \mathcal{F} \circ \mathcal{S}(\mathbf{p}^k)$.

2.2 Approximations for the inverse of the Jacobian

Resume by listing three suitable reduced order models for the approximation for the inverse of the Jacobian. In this section we will discuss the Gauss-Seidel method, Aitken's adaptive underrelaxation method, and the Least-Squares method.

The Gauss-Seidel method with subiterations, where the structure is solved first, is given by

$$\mathbf{d}^{k+1} = \mathcal{S}(\mathbf{p}^k), \tag{9a}$$

$$\mathbf{p}^{k+1} = \mathcal{F}(\mathbf{d}^{k+1}). \tag{9b}$$

Since we measure convergence of the pressure, it is useful to write it as

$$\mathbf{p}^{k+1} = \mathcal{F} \circ \mathcal{S}(\mathbf{p}^k), \tag{10}$$

and so the residual for the Gauss-Seidel method becomes

$$\mathbf{r}^k = \mathcal{R}(\mathbf{p}^k) = \mathcal{F} \circ \mathcal{S}(\mathbf{p}^k) - \mathbf{p}^k = \mathbf{p}^{k+1} - \mathbf{p}^k. \tag{11}$$

Combine (10) and (11) with (7) to find the expression for the approximation of the inverse of the Jacobian for the Gauss-Seidel method,

$$\overline{\left(\left. \frac{\mathrm{d}\mathcal{R}}{\mathrm{d}\mathbf{p}} \right|_{\mathbf{p}^k} \right)^{-1}}^{\mathrm{GS}} = -I. \tag{12}$$

Unfortunately for strong coupling problems, sub-iterations for the Gauss-Seidel method converge slow or even do not converge at all. A first step to overcome these problems is to introduce underrelaxation.

The Gauss-Seidel method often appears to be either very slow (needs many sub-iterations) or even unstable. A simple and already very effective way is to introduce some underrelaxation. First perform a structure and flow solve as was done in the previous section (10). Now the output will not directly be used as an input for the next subiteration, but an underrelaxation will be performed, which is a linear combination of the output and the state of the previous subiteration,

$$\mathbf{p}^{k+1} = \omega \tilde{\mathbf{p}}^{k+1} + (1-\omega)\mathbf{p}^k = \mathbf{p}^k + \omega \mathbf{r}^k. \tag{13}$$

The underrelaxation has a stabilizing effect on the convergence process. Aitken's underrelaxation method goes one step further, it uses an adaptive underrelaxation parameter ω^k, that is based on the one-dimensional Secant method. This Secant method uses a finite-difference approximation of the Jacobian. Suppose we want to solve the scalar equation

$\mathcal{R}(p) = 0$ using Secant's method, then

$$\begin{aligned} p^{k+1} &= p^k + \frac{p^k - p^{k-1}}{\mathcal{R}(p^k) - \mathcal{R}(p^{k-1})}\big(-\mathcal{R}(p^k)\big) \\ &= p^k + \frac{\omega^{k-1} r^{k-1}}{r^k - r^{k-1}}(-r^k) \\ &= p^k + \omega^k r^k. \end{aligned}$$

For a system with vectors the idea is the same except that it is not possible to divide by a vector. An innerproduct multiplication with $\mathbf{r}^k - \mathbf{r}^{k-1}$ is used instead. Aitken's approximation of the inverse of the Jacobian becomes

$$\overline{\left(\frac{\mathrm{d}\mathcal{R}}{\mathrm{d}\mathbf{p}}\bigg|_{\mathbf{p}^k}\right)^{-1}}_{\text{Aitken}} = -\omega^k I, \quad \text{with} \quad \omega^k = -\omega^{k-1}\frac{\big\langle(\mathbf{r}^{k-1}), (\mathbf{r}^k - \mathbf{r}^{k-1})\big\rangle}{\big\langle(\mathbf{r}^k - \mathbf{r}^{k-1}), (\mathbf{r}^k - \mathbf{r}^{k-1})\big\rangle}. \tag{14}$$

The Aitken method results in a recursive, single-diagonal, single-value approximation for the inverse of the Jacobian. The Aitken method is known to be very cheap, while a big increase in stability and a reduction in the number of subiterations are noticed.

Despite the capabilities of the Aitken method, it also has its limits. It weighs the residual of every node with the same factor, which results in a sub-optimal convergence. A method that weights each node differently is the least-squares[1] method [2]. The method is based on the reuse of the state and residual from previous subiterations, including that from previous timesteps, to make a linear extrapolation for the new state.

The method relies on a least-squares approximation of the difference between the newly retrieved data and residual, $\tilde{\mathbf{p}}^{k+1}$, $\tilde{\mathbf{r}}^k$ and a (large) number of previously obtained data and residual vectors, $\tilde{\mathbf{p}}^{i+1}$, $\mathbf{r}^i$, given by

$$\Delta\tilde{\mathbf{p}}^{i+1} = \tilde{\mathbf{p}}^{i+1} - \tilde{\mathbf{p}}^{k+1}, \tag{15a}$$

$$\Delta\mathbf{r}^i = \mathbf{r}^i - \mathbf{r}^k, \tag{15b}$$

for $i = 0, \ldots, k-1$. The desired change in residual vector, $\Delta\mathbf{r}^k = 0 - \mathbf{r}^k$, can be approximated by a linear combination of the known residual changes $\Delta\mathbf{r}^i$, as

$$\Delta\mathbf{r}^k \approx \sum_{i=1}^{k-1} c_i^k \Delta\mathbf{r}^i. \tag{16}$$

Because, in general, this gives an overdetermined system, for the coefficients $\mathbf{c}^k$, the system is solved as a minimization problem using the least-squares method,

$$\mathbf{c}^k = \arg\min \left\| \mathbf{r}^k + \sum_{i=1}^{k-1} c_i^k \Delta\mathbf{r}^i \right\|_2. \tag{17}$$

[1] also called IQN-ILS, Interface Quasi-Newton method with and approximation for the Inverse of the Jacobian using Least-Squares method.

Because $\Delta\tilde{\mathbf{p}}^k$ corresponds to $\Delta\mathbf{r}^k$, a similar linear combination as in (16) gives an approximation for $\Delta\tilde{\mathbf{p}}^k$,

$$\Delta\tilde{\mathbf{p}}^k \approx \sum_{i=1}^{k-1} c_i^k \Delta\tilde{\mathbf{p}}^i. \tag{18}$$

Finally, from (8) and (15) we find

$$\mathbf{p}^{k+1} - \mathbf{p}^k = \Delta\mathbf{p}^k = \Delta\tilde{\mathbf{p}}^k - \Delta\mathbf{r}^k \tag{19}$$

which gives us our new pressure state $\mathbf{p}^{k+1}$, by substituting (16) and (18), with coefficients found in (17).

Note that (17) may result in a QR-decomposition, applied to a matrix $\mathsf{V}^k = \mathsf{Q}^k\mathsf{R}^k$, whose columns are the vectors $\Delta\mathbf{r}^i$. Then (17) becomes

$$\mathsf{R}^k\mathbf{c}^k = \mathsf{Q}^{k^T}\Delta\tilde{\mathbf{r}}^k,$$

and so the approximation of the inverse of the Jacobian using the Least-Squares method is given by

$$\overline{\left(\left.\frac{\mathrm{d}\mathcal{R}}{\mathrm{d}\mathbf{p}}\right|_{\mathbf{p}^k}\right)^{-1}}_{\mathrm{LS}} = \mathsf{W}^k\mathsf{R}^{k^{-1}}\mathsf{Q}^{k^T} - I, \tag{20}$$

with W^k a matrix whose columns are the vectors $\Delta\tilde{\mathbf{p}}^i$. This gives a full matrix for the approximated inverse Jacobian, that is diagonally dominated.

3 MULTI-LEVEL ACCELERATION IN FSI

3.1 Derivation of coarse grid prediction method

Let $\mathbf{v}$ be a vector containing all structure variables, and let $\mathbf{w}$ be a vector containing all flow variables (i.e. (u, p) for incompressible and (ρ, u, p) for compressible flows). Let $\mathbf{d}$ be the displacement vector at the fluid-structure interface, Γ_I, and $\mathbf{p}$ be the pressure state on Γ_I. These are obtained by interpolating $\mathbf{v}$, respectively $\mathbf{w}$, towards the fluid-structure interface, using an interpolation function ϕ_{Γ_I}, i.e. $\mathbf{d} = \phi_{\Gamma_I}(\mathbf{v})$, $\mathbf{p} = \phi_{\Gamma_I}(\mathbf{w})$. Now define the following two (black-box) solvers:

$$\mathcal{S}(\mathbf{v}; \mathbf{p}) - \mathbf{s} = 0, \tag{21a}$$

$$\mathcal{F}(\mathbf{w}; \mathbf{d}) - \mathbf{f} = 0, \tag{21b}$$

where $\mathcal{S}$ and $\mathcal{F}$ are the implicit parts of the structure and flow solver, with $(a; b)$ their arguments, where a are the variables to be solved and b the input variables from the other solver(s). The vectors $\mathbf{s}$ and $\mathbf{f}$ are the explicit parts of the solvers. These do not change during coupling iterations. We make a distinction between quantities corresponding to a fine and coarse grid using the subscripts $_h$ and $_H$, respectively.

The fine grid solution is obtained by solving equations (21a) and (21b) in series. First solve for $\mathbf{v}_h^{k+1}$ using $\mathbf{p}_h^k$ as input, and obtain from that $\mathbf{d}_h^{k+1}$. Then use this interface displacement as input to obtain the flow state, $\tilde{\mathbf{w}}_h^{k+1}$ and corresponding pressure at the interface, $\mathbf{p}_h^{k+1}$.

$$\begin{cases} \mathcal{S}(\mathbf{v}_h^{k+1};\mathbf{p}_h^k) - \mathbf{s}_h^n = 0, \\ \mathcal{F}(\tilde{\mathbf{w}}_h^{k+1};\mathbf{d}_h^{k+1}) - \mathbf{f}_h^n = 0. \end{cases} \tag{22}$$

Equations (21) are not only used to solve for structure and flow variables, but can also be used in an evaluation to obtain structure and flow residuals. For that, substitute the solutions of the previous iteration,

$$\begin{cases} \mathbf{r}_{s,h}^k = \mathcal{S}(\mathbf{v}_h^k;\mathbf{p}_h^k) - \mathbf{s}_h^n, \\ \mathbf{r}_{f,h}^k = \mathcal{F}(\tilde{\mathbf{w}}_h^k;\mathbf{d}_h^{k+1}) - \mathbf{f}_h^n. \end{cases} \tag{23}$$

Now we can define the error of each quantity, $\epsilon_{\mathbf{v},h}^k = \mathbf{v}_h^{k+1} - \mathbf{v}_h^k$ and $\epsilon_{\tilde{\mathbf{w}},h}^k = \tilde{\mathbf{w}}_h^{k+1} - \tilde{\mathbf{w}}_h^k$. The system to solve becomes

$$\begin{cases} \mathcal{S}(\epsilon_{\mathbf{v},h}^k;\mathbf{0}) = -\mathbf{r}_{s,h}^k, \\ \mathcal{F}(\epsilon_{\tilde{\mathbf{w}},h}^k;\mathbf{0}) = -\mathbf{r}_{f,h}^k, \end{cases} \tag{24}$$

A similar system can be defined for the coarse grid,

$$\begin{cases} \mathcal{S}(\epsilon_{\mathbf{v},H}^k;\mathbf{0}) = -\mathsf{R}\mathbf{r}_{s,h}^k, \\ \mathcal{F}(\epsilon_{\tilde{\mathbf{w}},H}^k;\mathbf{0}) = -\mathsf{R}\mathbf{r}_{f,h}^k, \end{cases} \tag{25}$$

except that we use the reduction, performed by matrix R, of the fine grid residual to the coarse grid. Indeed the solution is fully coupled when the residuals $\mathbf{r}_{s,h}^k$ and $\mathbf{r}_{f,h}^k$ are zero and not when $\mathbf{r}_{s,H}^k$ and $\mathbf{r}_{f,H}^k$ equal zero. The reduction matrix is also used to obtain the states on the coarse grid,

$$\mathbf{v}_H^k = \mathsf{R}\mathbf{v}_h^k \quad \text{and} \quad \mathbf{w}_H^k = \mathsf{R}\mathbf{w}_h^k. \tag{26}$$

We can replace the errors by the difference between two solves,

$$\begin{cases} \mathcal{S}(\mathbf{v}_H^{k+1};\mathbf{p}_H^k) - \mathcal{S}(\mathbf{v}_H^k;\mathbf{p}_H^k) = -\mathsf{R}\mathbf{r}_{s,h}^k, \\ \mathcal{F}(\mathbf{w}_H^{k+1};\mathbf{d}_H^{k+1}) - \mathcal{F}(\mathbf{w}_H^k;\mathbf{d}_H^{k+1}) = -\mathsf{R}\mathbf{r}_{f,h}^k. \end{cases} \tag{27}$$

Finally write it in the form of (22), to obtain the method on the coarse grid level,

$$\begin{cases} \mathcal{S}(\mathbf{v}_H^{k+1};\mathbf{p}_H^k) - \mathbf{s}_H^{k+1} = 0 \quad \text{with} \quad \mathbf{s}_H^{k+1} = -\mathsf{R}\mathbf{r}_{s,h}^k + \mathbf{r}_{s,H}^k + \mathbf{s}_H^k \\ \mathcal{F}(\tilde{\mathbf{w}}_H^{k+1};\mathbf{d}_H^{k+1}) - \mathbf{f}_H^{k+1} = 0 \quad \text{with} \quad \mathbf{f}_H^{k+1} = -\mathsf{R}\mathbf{r}_{f,h}^k + \mathbf{r}_{f,H}^k + \mathbf{f}_H^k \end{cases} \tag{28}$$

Note that in the coarse grid formulation the terms $\mathbf{s}_H^{k+1}$ and $\mathbf{f}_H^{k+1}$ are no longer constant, but that there appears a recurrence relation.

The new structure state is obtained by a prolongation of the coarse grid correction,

$$\begin{aligned}\mathbf{v}_h^{k+1} &= \mathbf{v}_h^k + \mathsf{P}\epsilon_{\mathbf{v},H}^k \\ &= \mathbf{v}_h^k + \mathsf{P}(\mathbf{v}_H^{k+1} - \mathbf{v}_H^k)\end{aligned} \tag{29}$$

and the new fine grid states of the flow states are given using the following prolongation,

$$\tilde{\mathbf{w}}_h^{k+1} = \mathbf{w}_h^k + \mathsf{P}(\tilde{\mathbf{w}}_H^{k+1} - \mathbf{w}_H^k). \tag{30}$$

From $\tilde{\mathbf{w}}_h^{k+1}$ we can extract the pressure state at the fluid-structure interface, $\tilde{\mathbf{p}}_h^{k+1}$, using the map ϕ_{Γ_I}. Now calculate the approximate inverse Jacobian, $\mathcal{J}^{-1}$, with one of the methods discussed in the previous section, and apply the quasi-Newton step,

$$\mathbf{p}_h^{k+1} = \mathbf{p}_h^k + \mathcal{J}^{-1}(-\mathbf{r}^k), \tag{31}$$

where $\mathbf{r}^k = \tilde{\mathbf{p}}_h^{k+1} - \mathbf{p}_h^k$, so

$$\begin{aligned}\mathbf{p}_h^{k+1} &= \mathbf{p}_h^k + \mathcal{J}^{-1}\left(-\mathsf{P}\epsilon_H^k\right) \\ &= \mathbf{p}_h^k + \mathcal{J}^{-1}\left(-\mathsf{P}(\tilde{\mathbf{p}}_H^{k+1} - \mathbf{p}_H^k)\right).\end{aligned} \tag{32}$$

3.2 Multi-level convergence criteria

As mentioned in the introduction, a multi-level convergence criteria will be derived. The fine grid residual, $\mathbf{r}_F$, can be decomposed in a part corresponding to the coarse grid residual on the fine grid, $\mathbf{r}_C$, and high wave number residual term, $\boldsymbol{\delta}$, for which holds that it vanishes when restricting it to the coarse grid, $\mathsf{R}\boldsymbol{\delta} = 0$,

$$\mathbf{r}_F = \mathbf{r}_C + \boldsymbol{\delta}. \tag{33}$$

Note that compared to the previous section, we have $\mathbf{r}_F = \mathbf{r}_h$ and $\mathbf{r}_C = \mathsf{P}\mathbf{r}_H$, so both are defined w.r.t. the fine grid. As we subiterate on the coarse grid, we will notice that $\mathbf{r}_C \to 0$, while $\mathbf{r}_F \to \boldsymbol{\delta}$. The new multi-level convergence criteria is related to the ratio between the coarse grid residual and the high wave number residual,

$$\frac{\|\mathbf{r}_C\|}{\|\boldsymbol{\delta}\|} = \frac{\|\mathbf{r}_C\|}{\|\mathbf{r}_F - \mathbf{r}_C\|} \leq C. \tag{34}$$

A reasonable criteria is to set $C = 1$, in that case $\|\mathbf{r}_C\| \leq \boldsymbol{\delta}$. Then the remaining coarse grid residual is smaller than the high wave number residual, that cannot be removed on the coarse level. Therefore a prolongation to a finer grid seems reasonable.

Note that in practice the high wave number residual $\|\mathbf{r}_F - \mathbf{r}_C\|$ is not known, but the individual residuals, $\|\mathbf{r}_F\|$ and $\|\mathbf{r}_C\|$, are. Instead, we will measure a slightly higher value,

$$\frac{\|\mathbf{r}_C\|}{\|\mathbf{r}_F\| - \|\mathbf{r}_C\|} \geq \frac{\|\mathbf{r}_C\|}{\|\mathbf{r}_F - \mathbf{r}_C\|}. \tag{35}$$

4 NUMERICAL INVESTIGATION

The discussed reduces order models are applied to the cilinder with flapping beam benchmark case, version FSI3, introduced in [9]. The case shows transient behavior with large displacement and is strongly coupled, since the densities of the flow and structure are equal. Details of the used solvers can be found in [12]. Most important to mention here is that time integration is performed using the ESDIRK3 method, an implicit, third-order accurate, multistage Runge-Kutta scheme, see [11]. Each implicit Runge-Kutta stage is subiterated until $\|\mathbf{r}_h\| \leq 10^{-3}$. The coarse and fine grids are shown in figure 1. The ratio of fine to coarse grid is 20737 to 5442 cells, i.e. about 3.8.

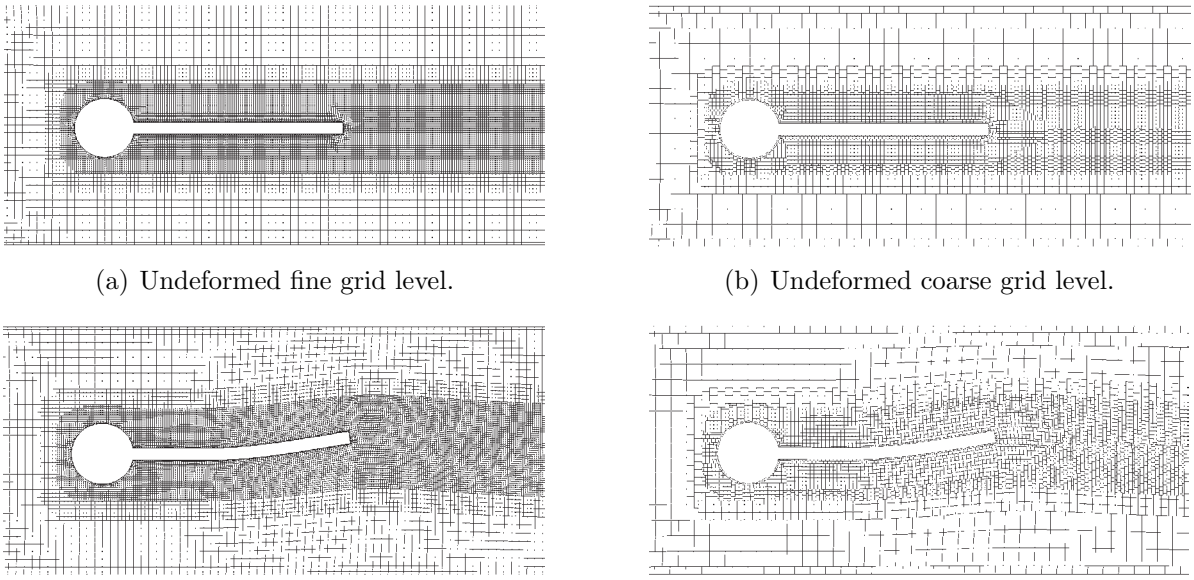

(a) Undeformed fine grid level.

(b) Undeformed coarse grid level.

(c) Deformed fine grid level.

(d) Deformed coarse grid level.

Figure 1: Fine and coarse level meshes for undeformed and deformed situation.

4.1 Results

A list of different multi-level strategies are tested in combination with Aitken and Least-squares quasi-Newton method:

- **FG:** Fine grid solves only.
- **∞CG-∞FG:** First iterate on coarse grid level until convergence, thereafter iterate on fine grid level until convergence.
- **2CG-1FG:** Alternate between two coarse grid solves with one fine grid solve. Final solve is always a fine grid solve.

Method		Total	Fine	Coarse
Aitken	FG	30.7 10.2	30.7 10.2	0.0 0.0
Least-squares	FG	20.7 6.9	20.7 6.9	0.0 0.0
Aitken	∞CG-∞FG	56.6 18.9	21.2 7.1	35.4 11.8
Least-squares	∞CG-∞FG	42.7 14.2	18.4 6.1	24.3 8.1
Aitken	2CG-1FG	36.4 12.1	12.5 4.2	23.9 8.0
Least-squares	2CG-1FG	30.5 10.2	10.7 3.6	19.8 6.6
Aitken	3CG-1FG	38.2 12.7	10.3 3.4	27.9 9.3
Least-squares	3CG-1FG	35.1 11.7	9.5 3.2	25.6 8.5
Aitken	adaptive $C = 1.0$	36.4 12.1	12.2 4.1	24.2 8.1
Least-squares	adaptive $C = 1.0$	27.4 9.1	10.8 3.6	16.6 5.5
Aitken	adaptive $C = 0.5$	39.2 13.1	10.9 3.6	28.3 9.4
Least-squares	**adaptive C = 0.5**	**29.4 9.8**	**9.2 3.1**	**20.2 6.7**

Table 1: Average number of subiterations for 100 timesteps. In black: average per timestep. In blue: average per implicit RK stage.

- **Adaptive C = 0.5:** Adaptively alternate between coarse grid solves with fine grid solves. Final solve is always a fine grid solve.

The results are given in table 1. It shows the average number of subiterations taken over 100 timesteps. It show both the average number per timestep as well as per implicit Runge-Kutta stage. With respect to fine grid solves only, the ∞CG-∞FG method shows a major increase in total number of subiterations and only a minor decrease in the expensive fine grid solves. The alternating method 2CG-1FG also has an increase in total number of subiteractions, but the number of fine grid subiterations is already halved. Finally the adaptive multi-level method with $C = 0.5$ shows the best result. With respect to fine grid level only, a minor increase in total number of subiteractions is noticed, while there is a major decrease in fine grid solves. Per implicit RK stage, the number of fine grid solves reduces from 10.2 to 3.6 when using Aitken's method, and from 6.9 to 3.1 when using least-squares method.

4.2 Convergence behavior

Figure 2 shows the convergence behavior for a full timestep of Aitken's and least-squares method using fine grid level only, and the least-squares method with adaptive multi-level strategy. Most important to see is that for the first five subiterations each stage, the multi-level approach has the same convergence behavior as the fine grid level only approach. Only for the last few subiterations the convergence ratio is less for the multi-level approach than for the fine grid level only approach.

To indicate the existence of $\boldsymbol{\delta}$, we compare the convergence behavior of the ∞CG-∞FG strategy with both Aitken and least-squares, with the convergence of least-squares adap-

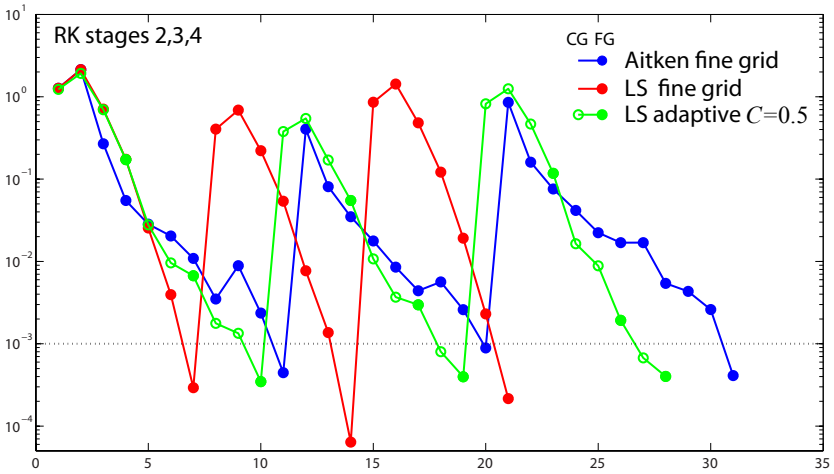

Figure 2: Convergence behavior of a typical timestep.

tive multi-level $C = 0.5$, see figure 3. The ∞CG-∞FG methods show a clear jump when switching from coarse to fine level. Both Aitken and Least-squares method jump almost to the same level. This clearly indicates that although convergence on the coarse grid has been reached, there remains to exists a high frequency mode, $\boldsymbol{\delta}$, that cannot be suppressed by the coarse level solves. This mode is indeed recognized by the adaptive multi-level strategie, which therefore uses a finegrid solve just above the $\boldsymbol{\delta}$-level, to suppress this mode.

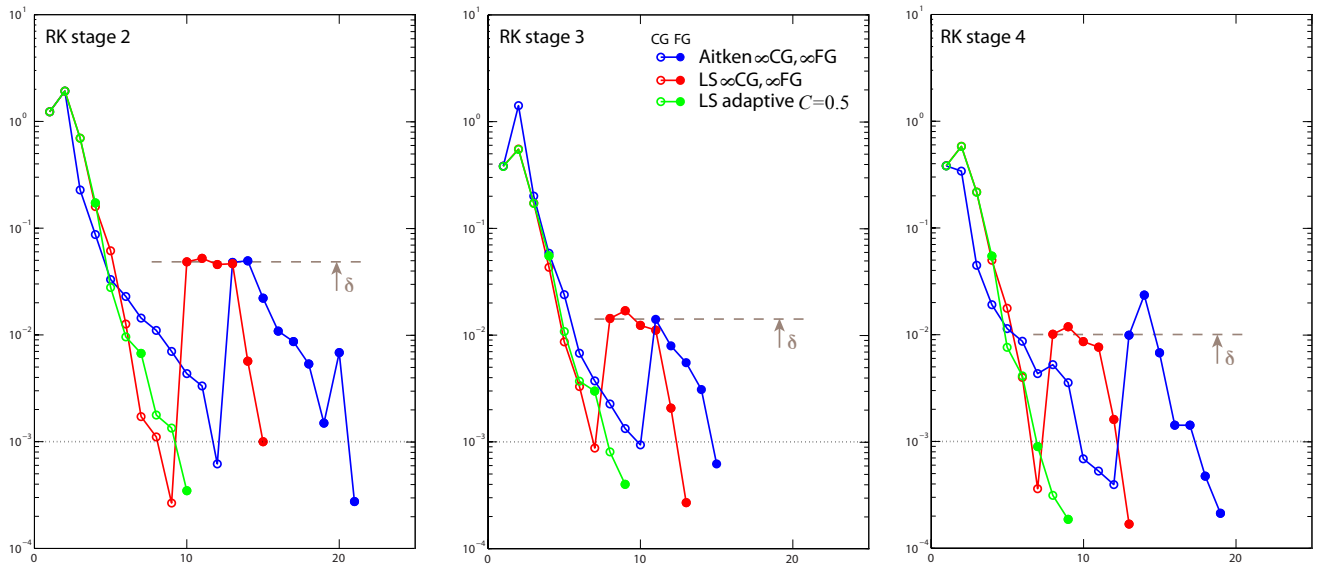

Figure 3: Convergence behavior of a typical timestep, that indicates the existence of the high frequency mode, $\boldsymbol{\delta}$.

REFERENCES

[1] E.H. van Brummelen, C. Michler and R. de Borst, "Interface-GMRES(R) acceleration of subiteration for fluid-structure-interaction problems", Technical Report *Delft Aerospace Computational Science*, (2005), DACS-05-001.

[2] J. Degroote, R. Haelterman, S. Annerel, P. Bruggeman, J. Vierendeels, "Performance of partitioned procedures in fluid-structure interaction", *Computers & Structures*, (2010), **88**, 446-457.

[3] J. Degroote, S. Annerel and J. Vierendeels, "Stability analysis of Gauss-Seidel iterations in a partitioned simulation of fluid-structure interaction", *Computers & Structures*, (2010), **88**, 5-6, 263-271.

[4] C. Farhat, K. van der Zee and P. Geuzaine, "Provably second-order time-accurate loosely coupled solution algorithms for transient nonlinear computational aeroelasticity", *Comp. Meth. in Appl. Mech. and Eng.*, (2006), **195**, 17-18, 1973-2001.

[5] T. Gallinger and K. Bletzinger, "Comparison of algorithms for strongly coupled partitioned fluid-structure interaction - Efficiency versus simplicity", *Proceeding ECCOMAS CFD 2010*.

[6] U. Küttler and W. Wall, "Fixed-point fluid-structure interaction solvers with dynamic relaxation", *Computational Mechanics*, (2008), **43**, 1, 61-72.

[7] C. Michler, E.H. van Brummelen and R. de Borst, "An interface Newton-Krylov solver for fluid-structure interaction, *International Journal for Numerical Methods in Fluids*, (2005), **47**, 10-11, 1189-1195.

[8] S. Piperno, C. Farhat, B. Larrouturou, "Partitioned procedures for the transient solution of coupled aeroelastic problems. Part I: model problem, theory and two-dimensional application", *Comp. Meth. Appl. Mech. Eng.*, (1995), **124**, 1-2, 79-112.

[9] S. Turek, J. Hron, in *Fluid-Structure Interaction: Modelling, Simulation, Optimisation*, ed. by H.J. Bunggartz, M. Schaefer, Springer, (2006).

[10] A.H. van Zuijlen, S. Bosscher, H. Bijl, "Two level algorithms for partitioned fluid-structure interaction computations", *Comp. Meth. Appl. Mech. Eng.*, (2007), **196**, 1458-1470.

[11] A.H. van Zuijlen, A. de Boer and H. Bijl, "Higher-order time integration through smooth mesh deformation for 3D fluid-structure interaction simulations", *Journal of Computational Physics*, (2007), **224**, 1, 414-430.

[12] A.H. van Zuijlen and H. Bijl, "Multi-level accelerated sub-iterations for fluid-structure interaction", in *FSI II*, Lecture notes Comp. Sc. Eng., (2010), **73**, 1-25.